

Aerothermoelastic Response of a Functionally-Graded Aircraft Wing to Heat Loads

F. Mastroddi^a, G.M. Polli^b, A. Argiolas^a, N. Di Matteo^a

^a “Sapienza” - Università di Roma
Dipartimento di Ingegneria Aerospaziale

^b C.R. ENEA Frascati
Superconductivity Division

Abstract

In this paper, a coupled aerothermoelastic dynamic stability analysis of a functionally-graded composite wing including non-classical effects, and immersed in a gas flow is developed. Specifically, the study concerns the aerothermoelastic stability of aircraft swept wings made of advanced functionally-graded composite materials and exposed to a heat flow impacting its deformed surface. The structural model is specialized in the computations to the case of a rectangular, single-layered, swept wing made of functionally graded material (FGM) with a ceramic-metallic-ceramic phase gradient. In particular, aluminum and alumina have been chosen as metallic and ceramic phases respectively. The evaluation of the temperature field on the deformed (actual) configuration of the wing permits to address the problems of the aerothermoelastic response and stability in a coupled framework. As a result, the exact analytical expression of the aerothermoelastic response of the heated wing is obtained in the Laplace space domain and, following this, the static and dynamic aeroelastic instabilities of the wing model are determined. The obtained results indicate that the aeroelastic stability is substantially affected by the thermo-elastic coupling and that the presence of FGM can also significantly influence the aerothermoelastic behaviour. In the discussion of the results, special attention is given to the effects played by the flight speed and thermal anisotropy of the constituent material in terms of possible different FGM configurations.

1. Introduction

Recent activities related to space exploration and the renewed interest in supersonic/hypersonic flight vehicles, [1–4] require a good understanding of the aeroelastic instability and response of aeronautical/aerospace vehicle structures operating in high temperature field. While the thermoelastic dynamic response and stability of trusses and beam structures (motivated by the experience in space flight applications) has been widely investigated, [5–10] to the authors’ best knowledge, theoretical analyses are not so developed in the field of aeronautical structures immersed in a flow field. Nonetheless, the importance of the aerothermoelastic response and stability analyses of aerospace systems has been largely recognized [11] (especially with respect to reusable launch vehicles), and, in this sense, a number of studies have been conducted to investigate the aerothermoelastic stability of aerospace vehicles by using CFD approaches for the aerodynamics and FE models for the structures. [1–4] In this context, this study presents an exact coupled aerothermoelastic stability analysis for heated com-

posite aircraft wings as proposed in Ref. [12]. In this Reference the study of the aerothermoelastic stability of aircraft swept wings made of advanced homogeneous composite materials, exposed to a generic heat flow field and operating in an incompressible flow was addressed. The thermal field is supposed to be generated by a laser beam impacting the upper surface of the wing, Refs. [13, 14]. The use of a laser beam to produce thermal effects was motivated by the fact that this represents an actual way to impose in practice significant heat flows to a wing in operative conditions with an intensity so large to induce relevant aerothermoelastic effects. The wing structural model, previously developed by the authors, [13–16] is specialized in the present paper to the case of a rectangular, single-layered swept wing composed of a ceramic-metallic-ceramic FGM: to this purpose an analytic formulation for determining the thermal field in the material with non-homogeneous thermal characteristics is proposed.

In the numerical applications, aluminum has been chosen as core metal for the wing because of its massive use as structural material in aerospace applications, whilst alumina (Al_2O_3) has been chosen as a ceramic cover due to its good performance as a thermal shield

and its chemical constitutive affinity to aluminum.

The methodology adopted, based on the use of a double Laplace transform, was originally developed in Ref. [17] to solve the static aeroelastic response, then employed in Refs. [13–15, 18] to determine the flutter and divergence speed of swept composite wing structure, and in Refs. [13, 14, 19] to solve the aerothermoelastic dynamic response of the structure. In Reference [12] the formulation has been extended to the solution of an arbitrary dynamic aerothermoelastic coupled response. In the present paper the solution has been extended in order to include the FGM characterization. More specifically, a time-domain formulation of the theory of lifting surfaces was considered to model the unsteady aerodynamics. [20, 21] Moreover, the evaluation of the temperature field on the deformed (actual) configuration of the wing allows to address the problem of the aerothermoelastic response and stability in a coupled framework (see Ref. [12]; see also [13, 14] for a presentation of a similar analysis in an un-coupled regime). As a result, the exact analytical expression of the aerothermoelastic response of the FGM heated aircraft wing is obtained in the Laplace transformed space and, consequently, the stability boundary of the wing model is derived. In order to validate the results obtained in terms of aerothermoelastic flutter boundary, the thermoelastic static and dynamic stability analysis was presented in Refs. [12, 13] and the results are then compared with those available in literature for the aeroelasticity of homogeneous wings, Refs. [6–9]. In the presentation and discussion of the results, particular emphasis is placed on the effects of the FGM, of flight speed, thermal anisotropy and direction of the external heat flux impacting the wing surface.

2. Structural and aeroelastic model

The wing structure is modelled as a plate-like body with appropriate internal constraints (Fig.1). Specifically, it is assumed that the wing cross-sections are undeformable, and that the wall thickness is inextensible. As a result, the displacement field of the wing is represented by the following map [15, 16]

$$\begin{aligned} \mathbf{u}(\mathbf{x}, t) = & x_3 \theta(x_2, t) \mathbf{e}_1 + \{u_2 + x_3 [\beta(x_2, t) \\ & + x_1 g(x_2, t)]\} \mathbf{e}_2 + \{h(x_2, t) - [x_1 \\ & - x_0(x_2, t)] \theta(x_2, t)\} \mathbf{e}_3 \end{aligned} \quad (1)$$

where $u_2(x_2, t)$ is the extension in the spanwise direction, $\theta(x_2, t)$ denotes the twist angle of the wing about its pitching axis, $\beta(x_2, t)$ identifies the flexural angle about the chord-wise direction, $g(x_2, t)$ represents the warping displacement (see Fig.2), $h(x_2, t)$ denotes the plunging displacement of the wing cross section measured at the elastic axis (positive upward and located at $x_{1e} = x_0(x_2)$, Fig.1). Collecting the independent displacement components in Eq.(1), one may observe

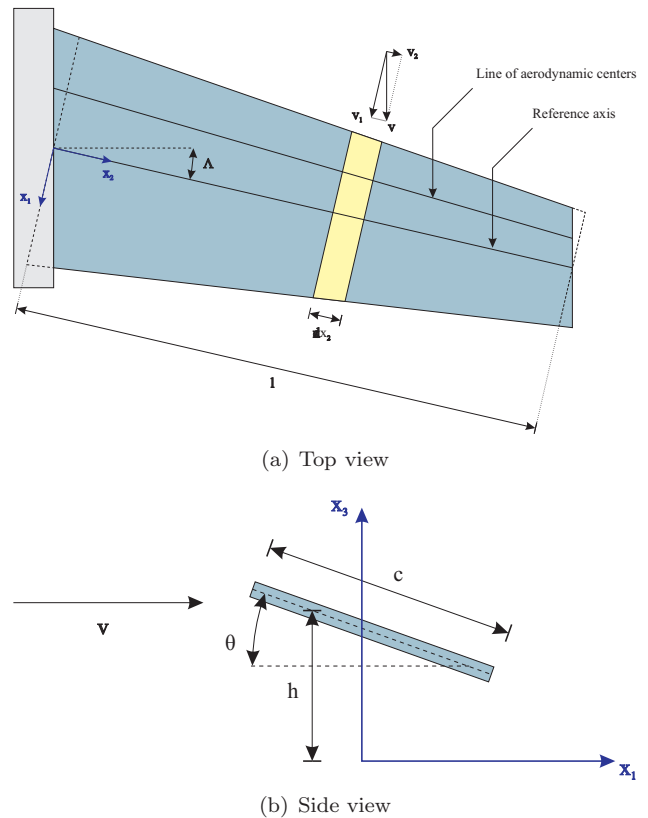


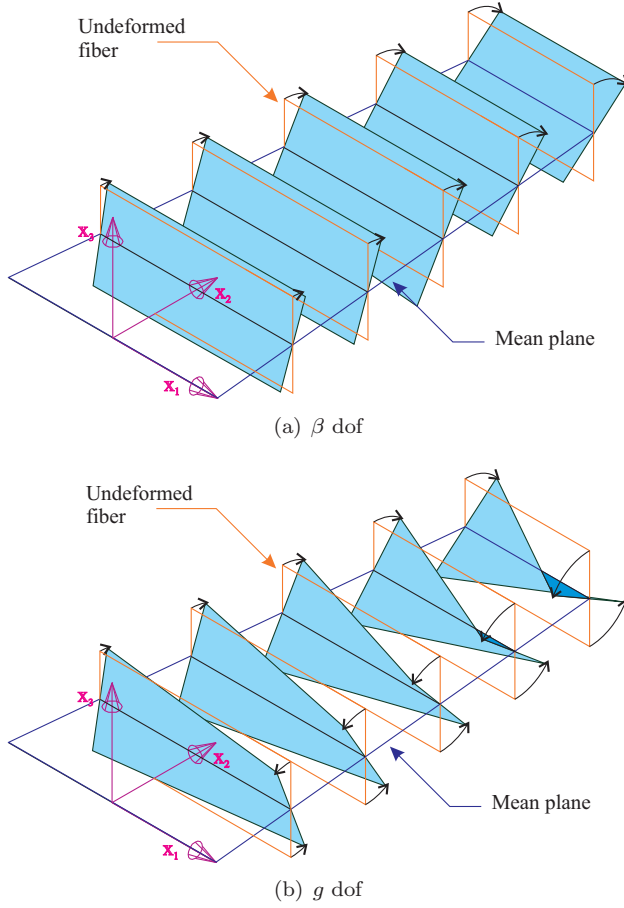
Figure 1. Geometry of the swept wing

that the total number of unknowns retained into the model is five, and in terms of these five displacement unknowns (u_2, β, g, θ, h) the aeroelastic response analysis under the effect of a thermo-mechanical load is investigated.

In order to be reasonably self-contained, the equilibrium equations and the related boundary conditions for a transversely isotropic swept aircraft wing, obtained via the application of Hamilton's principle, are shortly reviewed (the interested reader is referred to Refs. [12–16] for a complete presentation of this model). Specifically, denoting by $\mathbf{y} (= \{u_2, \beta, g, \theta, h\})$ the vector of the displacement unknowns, with \mathbf{K} , \mathbf{L} , \mathbf{P} the stiffness matrices, and with \mathbf{M} the mass matrix (their expressions are reported in Refs. [13, 14, 19]), in a condensed form, the equilibrium equations may be written as

$$\mathbf{K}\mathbf{y}'' + \mathbf{L}\mathbf{y}' + \mathbf{P}\mathbf{y} + \mathbf{M}\ddot{\mathbf{y}} = \mathbf{f}^A + \mathbf{f}^T + \mathbf{f}^M \quad (2)$$

where the primes ($'$) and the overdots ($\ddot{}$) denote the derivatives with respect to the spanwise coordinate x_2 and time t , respectively, whereas \mathbf{f}^A is the vector of aerodynamic loads, \mathbf{f}^T is the vector of thermal loads introduced by means of the constitutive equations, and \mathbf{f}^M is the vector of the generic mechanical loads that can act during the operational life of the vehicle (*e.g.*,

Figure 2. β and g degree of freedom

explosive blast, sonic-boom, gusts, *etc.*).

2.1. Constitutive equations for FGM materials

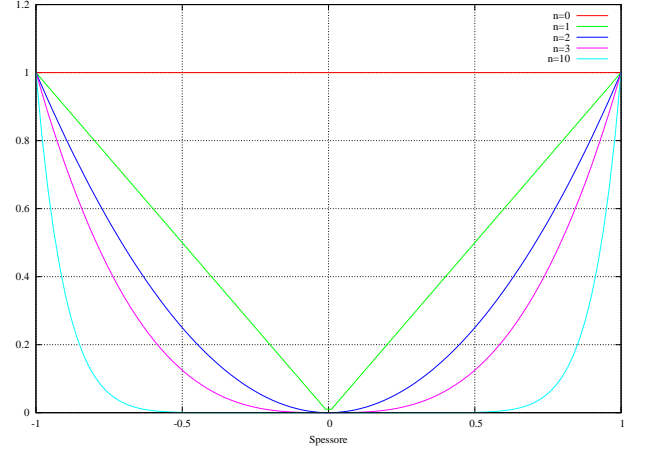
The FGM structure of the wing can be considered transversely isotropic, with the isotropy planes stacked in direction x_3 . It is supposed that the variation of a generic property P throughout the thickness could be expressed as

$$P(x_3) = [(1 - a_0)\mathcal{V}(x_3) + a_0](P_{ext} - P_{int}) + P_{ext} \quad (3)$$

where P_{ext} , P_{int} are the properties of the external and internal material component respectively, a_0 is the volumetric ratio on the mean plane, and $\mathcal{V}(x_3)$ is the law of volumetric variation of the FGM structure, and can assume values in the range $[0; 1]$, Ref. [22], according to

$$\mathcal{V}(x_3) = \left(\frac{x_3}{x_3^u}\right)^{n_u} \frac{1 + \text{Sgn}(x_3)}{2} + \left(\frac{x_3}{x_3^l}\right)^{n_l} \frac{1 - \text{Sgn}(x_3)}{2} \quad (4)$$

where x_3^u , x_3^l are the coordinates of the upper and lower surfaces of the wing, while the exponents n_u , n_l regulate the trend of volumetric fraction on the upper and lower part of the wing respectively (see Fig.3).

Figure 3. $\mathcal{V}(x_3)$ as a function of n_u , n_l

The constitutive matrix for a transversely isotropic linearly elastic material relating the six essential component of the strain tensor with the six ones of the stress tensor is given by

$$\mathbb{S} = \begin{bmatrix} \frac{1}{E_p} & -\frac{\nu_p}{E_p} & -\frac{\nu_{zp}}{E_z} & 0 & 0 & 0 \\ -\frac{\nu_p}{E_p} & \frac{1}{E_p} & -\frac{\nu_{zp}}{E_z} & 0 & 0 & 0 \\ -\frac{\nu_{pz}}{E_p} & -\frac{\nu_{pz}}{E_p} & \frac{1}{E_z} & 0 & 0 & 0 \\ 0 & 0 & 0 & \frac{1}{2G_{zp}} & 0 & 0 \\ 0 & 0 & 0 & 0 & \frac{1}{2G_{zp}} & 0 \\ 0 & 0 & 0 & 0 & 0 & \frac{1+\nu_p}{E_p} \end{bmatrix} \quad (5)$$

where the subscript p denotes the properties in the plane of isotropy and the subscript z the properties in the orthogonal plane. This formulation is still valid in the case of FGM, providing the following functional dependency for the elastic parameters: $E_p(x_3)$, $E_z(x_3)$, $G_{zp}(x_3)$, $\nu_p(x_3)$, $\nu_{pz}(x_3)$, and $\nu_{zp}(x_3)$. Since all the quantities in the used laminate formulation are integrated along the thickness, the dependence from x_3 will disappear from the structural matrices of the system.

2.2. Aerodynamic and thermal loads

The aerodynamic load vector is based on an incompressible, unsteady aerodynamic model which takes into account the effect of the sweep angle. It can be written in the following compact form [12–14, 19]

$$\mathbf{f}^A(\mathbf{y}, \dot{\mathbf{y}}, \ddot{\mathbf{y}}, \mathbf{y}', \dot{\mathbf{y}}') = \mathbf{A} \ddot{\mathbf{y}} + \mathbf{B} \dot{\mathbf{y}} + \mathbf{C} \mathbf{y}' + \mathbf{D} \dot{\mathbf{y}}' \quad (6)$$

$$+ \mathbf{E} I[\ddot{\mathbf{y}}(\hat{t}), t] + \mathbf{F} I[\dot{\mathbf{y}}(\hat{t}), t] + \mathbf{G} I[\mathbf{y}'(\hat{t}), t]$$

where $I[\bullet, t] := \int_0^t \varphi(t - \hat{t}) \bullet d\hat{t}$ and $\varphi(t)$ is the Wagner's function, [20, 21] whereas \mathbf{A} , \mathbf{B} , \mathbf{C} , \mathbf{D} , \mathbf{E} , \mathbf{F} , \mathbf{G} are the matrices of the aerodynamic coefficients whose expressions are reported in Refs. [13, 14, 19]. The functional representation of the vector of thermal loads will be supplied in the following section, and, in particular,

the explicit dependence of this load vector in terms of the unknown displacements. For the moment, let us note that using the modified Hooke-Duhamel constitutive equations (*e.g.*, Ref. [15]), and assuming a rectangular cross-section for the wing, the vector of thermal loads has only two non-zero component which does work on the extension $u_2(x_2, t)$ and flexural deflection of the wing $\beta(x_2, t)$, namely

$$\mathbf{f}^T(x_2, t) = \begin{bmatrix} \Theta_2^{0,0}(x_2, t) \\ \Theta_2^{0,1}(x_2, t) \\ 0 \\ 0 \\ 0 \end{bmatrix} \quad (7)$$

where $\Theta_2^{i,j}(x_2, t)$ is the thermal moment, whose expression will be explicited in the following section. For the forthcoming developments, it is convenient to define the vector of thermal moments as the derivative of a vector \mathbf{c} as follows (see Eq.(7))

$$\mathbf{f}^T(x_2, t) = \mathbf{c}'(x_2, t) \quad (8)$$

Therefore, the imposed boundary conditions at the root and the natural boundary conditions at the tip may be written

$$\mathbf{y}(0, t) = \mathbf{0} \quad (9)$$

$$\mathbf{R} \mathbf{y}'(L, t) + \mathbf{S} \mathbf{y}(L, t) = \mathbf{c}(t) \quad (10)$$

where L is the wing tip coordinate and where the boundary load \mathbf{c} reduces in our applications to a concentrated thermal moment acting on the flexural deflection of the wing. Equation (2) constitutes a system of four differential equations in space and time of the second order, whose boundary conditions are represented by Eqs.(9)-(10). In order to render the thermal load vector (\mathbf{f}^T) dependent on the state-space vector (\mathbf{y}) and on its derivatives, in a way similar to that of the aerodynamic load vector (see Eq.(6)), the thermal field has to be evaluated in the deformed configuration of the wing. This idea, together with the analytical evaluation of the thermal field for a FGM, is carried out in the following section.

3. Thermo-mechanical model for FGM

As already stated, the present formulation is carried out in the framework of coupled thermoelasticity, in the sense that the temperature distribution on the wing structure is supposed to be affected by the actual deformation of the structure. Moreover, it is assumed that the external heat input is generated by a laser beam impacting the upper surface of the wing, and finally the wing is treated as a solid parallelepiped. The problem may be mathematically stated in terms of the

following system of equations, Refs. [5, 13],

$$\text{Div}(\mathbf{K}\nabla T) - \rho c_t \frac{\partial T}{\partial t} = 0 \quad (11)$$

$$\mathbf{K}\nabla T \cdot \mathbf{n} = \mathbf{q} \cdot \mathbf{n} \quad (12)$$

$$\nabla T \cdot \mathbf{n} = 0 \quad (13)$$

$$T = 0 \quad (14)$$

where $T(\mathbf{x}, t)$ is the temperature field, \mathbf{K} is the thermal conductivity tensor, [23] ρ is the volume density, c_t is the specific heat, \mathbf{n} is the external normal to the surface body and \mathbf{q} is the external heat flux impacting the wing, moreover, Eq. 11 is the governing Fourier's law in the body, Eqs. 12-13 are the boundary conditions on the upper surface (where the heat input are applied) and elsewhere respectively, and Eq. 14 is the initial condition for the problem.

In order to encompass the variation through the thickness of the material properties according to Eq. 4, the behaviour of the generic thermal property $P(x_3)$ will be expressed as

$$P(z) = P_0 + P_v(z) \quad (15)$$

where P_0 is constant along the thickness and $P_v(x_3)$ is the varying part.

The temperature distribution within the body due to the application of the external heat inputs has been obtained adopting the Green's influence function approach suitably modified to take into account the functional dependence of the coefficients introduced by the FGM. In particular, the adjoint problem, needed to determine the influence function, has been solved with respect to the uniform part of the problem and then it has been used to solve the original non-uniform formulation (the reader is referred to Ref. [14] for further details).

Using the previous equation, an explicit relation between the temperature field and the unknown displacement components can be established. Indeed, the unit normal to the deformed upper surface of the wing is expressed in terms of a linear approximation involving the actual plunge and pitch of the wing, Refs. [13, 14, 19],

$$\mathbf{n}(\mathbf{x}, t) \cong \mathbf{e}_3 - h'(x_2, t) \mathbf{e}_2 + \theta(x_2, t) \mathbf{e}_1 \quad (16)$$

As a result, representing the heat flux vector in terms of its components on the Cartesian reference system chosen (*i.e.*, $\mathbf{q}(\mathbf{x}, t) = \{q_1(\mathbf{x}, t), q_2(\mathbf{x}, t), q_3(\mathbf{x}, t)\}$), the temperature field may be written as the sum of three terms. The first term ($T_1(\mathbf{x}^*, t)$) depends on the actual pitch displacement of the wing ($\theta(x_2, t)$), and

its expression is given by

$$T_1(\mathbf{x}^*, t^*) = - \int_0^{t^*} \sum_{n, \mathbf{m}, \mathbf{k}} \frac{8}{x_2 \bar{z}} W_{\mathbf{m}n} W_{\mathbf{k}n} \frac{1}{b_n} e^{\frac{a_n}{b_n}(t^* - t)} q_1(t) \cos\left(\frac{p\pi x_1^*}{\bar{x}}\right) \cos\left(\frac{q\pi x_2^*}{\bar{x}}\right) \cos\left(\frac{r\pi z^*}{\bar{z}}\right) \cos\left(\frac{w\pi z}{\bar{z}}\right) \int_0^{\bar{y}} \theta(x_2, t) \cos\left(\frac{j\pi x_2}{\bar{y}}\right) dx_2 dt \quad (17)$$

where q_1 is the component of the heat density vector (\mathbf{q}) in the chordwise x_1 direction. Note that in the previous formula the bold index \mathbf{m} is assumed to count the same quantities as the triple index' i, j , and w (in this case $j = 0$ to have integral not equal to zero) whereas, in a similar way, the bold index \mathbf{k} counts the same quantities of the triple index' p, q , and r . The second term $T_2(\mathbf{x}^*, t)$ depends on the actual bending of the wing ($h'(x_2, t)$) and its expression is given by

$$T_2(\mathbf{x}^*, t^*) = \int_0^{t^*} \sum_{n, \mathbf{m}, \mathbf{k}} \frac{8}{\bar{y}\bar{z}} W_{\mathbf{m}n} W_{\mathbf{k}n} \frac{1}{b_n} e^{\frac{a_n}{b_n}(t^* - t)} q_2(t) \cos\left(\frac{p\pi x_1^*}{\bar{x}}\right) \cos\left(\frac{q\pi x_2^*}{\bar{y}}\right) \cos\left(\frac{r\pi x_3^*}{\bar{z}}\right) \cos\left(\frac{w\pi x_3}{\bar{z}}\right) \int_0^{\bar{y}} h'(x_2, t) \cos\left(\frac{j\pi x_2}{\bar{y}}\right) dx_2 dt \quad (18)$$

where q_2 is the component of the heat density vector (\mathbf{q}) in the spanwise x_2 direction (the same assumption as before has been done for the bold index).

The third term ($T_3(\mathbf{x}, t)$) does not depend on the state-space vector and represents the uncoupled temperature field already employed in Ref. [13, 14] to perform a thermo-aeroelastic response analysis of the same wing model, and its expression is

$$T_3(\mathbf{x}^*, t^*) = - \int_0^{t^*} \sum_{n, \mathbf{m}, \mathbf{k}} \frac{8}{\bar{z}} W_{\mathbf{m}n} W_{\mathbf{k}n} \frac{1}{b_n} e^{\frac{a_n}{b_n}(t^* - t)} q_3(t) \cos\left(\frac{p\pi x_1^*}{\bar{x}}\right) \cos\left(\frac{q\pi x_2^*}{\bar{y}}\right) \cos\left(\frac{r\pi x_3^*}{\bar{z}}\right) \cos\left(\frac{w\pi x_3}{\bar{z}}\right) dt \quad (19)$$

where q_3 is the component of the heat density vector (\mathbf{q}) in the thickness x_3 direction (the same assumption as before has been done for the bold index; moreover, also the j index give non-zero contribution only if $j = 0$).

In order to illustrate pictorially the idea behind this approach, in Fig.4, from Ref. [12], a snapshot of the deformed configuration of the wing impacted by a generic heat density vector \mathbf{q} is presented. From this figure it becomes apparent how the heat flux absorbed by the wing can depend on its actual deformation and as a result, the temperature field on the state-space vector. Finally, it is worth pointing out that the temperature in Eqs.(17)-(18) is a function of space and time

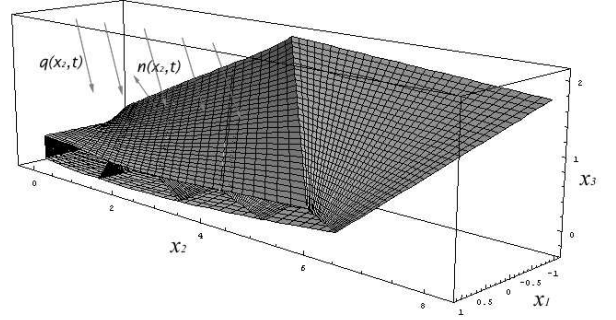


Figure 4. Effect of the aeroelastic deformation on the wing structure.

by means of the actual state-space vector, even if the heat density vector is supposed to be constant in space and time as it will be assumed later in the application.

Using Eqs.((17)-(19)), the thermal moment can be made dependent on the vector of displacement unknowns. Specifically, it is possible to write the thermal moment in the following compact form

$$c(y, y', x_2, t) = \sum_{m=0}^{\infty} \int_0^t U(m, x_2, t - t^*) \int_0^L [U_1(m, x_2^*, t^*) y(x_2^*, t^*) + U_2(m, x_2^*, t^*) y'(x_2^*, t^*)] dx_2^* dt^* + c_3(t) \quad (20)$$

where c_3 denotes the contribution to the thermal load vector due to Eq.(19), whereas U , U_1 and U_2 are three matrix operators whose definition can be deduced from the expression of the evaluated temperature field for FGM. Note that because of the particular geometry of the wing, the thermal moment induced by the heat flux in the x_3 direction reduces to a function of time only, once the heat flux q_3 is assumed constant in space. Indeed, in the contribution to the temperature field T_3 , the integrals of the eigenfunctions are all zero except for $l = m = 0$, thus this term reduces to a function of x_3 and t only. The functional dependence on the co-ordinate x_3 is successively eliminated by the integration across the wing cross-section of the thermal moment. Note also that the state-space vector y appears in the previous expression under the integral sign. There is, indeed, a convolution between the thermal input and the displacement field. The description of the procedure used to deal with this integral constitutes a significative part of the next section. Before proceeding further, it is remarkable to point out that in the solution of the aero-thermo-elastic problem an important role will be played by a parameter (B) [5] representing the ratio t_T/t_M between the characteristic thermal time ($t_T = \rho c_t H^2/k_3$) and a characteristic mechanical time (for instance the first natural bending

period). As it is stated in Ref. [5], the dynamic coupling increases as B becomes smaller. On the other hand, as B becomes larger the dynamic coupling disappears and the static solution alone remains valid.

4. Solution procedure

Following Refs. [13, 14, 19], the system of equilibrium equations (Eqs.(2)) with the associated boundary conditions (Eqs.(9)-(10)) can be reduced to a system of algebraic equations in Laplace space and time domains, where both the space and time coordinates are converted to their Laplace variable space counterparts. Indeed, applying the Laplace transform with respect to time to Eq.(2), and assuming zero initial conditions one has

$$\mathbf{K}\tilde{y}' + \tilde{\mathbf{N}}(s, U)\tilde{y}' + \tilde{\mathbf{Q}}(s, U)\tilde{y} = \tilde{f}^T(x_2, s) + \tilde{f}^M(x_2, s) \quad (21)$$

where the tilde ($L_t[\bullet] \equiv \tilde{\bullet}$) denotes the Laplace transform with respect to time, s is the Laplace variable representing the time counterpart of the physical space, whereas $\tilde{\mathbf{N}}$ and $\tilde{\mathbf{Q}}$ are two matrix operators that take into account the aerodynamic coupling and are given by

$$\tilde{\mathbf{N}}(s, U) := \mathbf{L} - \mathbf{C} - s\mathbf{D} - s\tilde{\varphi}\mathbf{G} \quad (22)$$

$$\tilde{\mathbf{Q}}(s, U) := \mathbf{N} + s^2(\mathbf{M} - \mathbf{A} - \tilde{\varphi}\mathbf{E}) - s(\mathbf{B} + \tilde{\varphi}\mathbf{F}) \quad (23)$$

where $\tilde{\varphi}$ is the Laplace transform of the Wagner's function and it is given by

$$\tilde{\varphi} := L_t[\varphi(t)] = \frac{C(s)}{s} \quad (24)$$

where C is the Laplace transform of Theodorsen's function.

Similarly, performing the Laplace transform with respect to space, and recalling that the wing is considered to be clamped at the root cross-section, one has

$$\hat{\tilde{y}}(p, s) = \left[p^2\mathbf{K} + p\tilde{\mathbf{N}}(s, U_n) + \tilde{\mathbf{Q}}(s, U_n) \right]^{-1} \begin{bmatrix} -\hat{\tilde{f}}^T(p, s) - \hat{\tilde{f}}^M(p, s) + \mathbf{K}\tilde{y}'(0, s) \end{bmatrix} \quad (25)$$

where the overhat ($L_{x_2}[\bullet] \equiv \hat{\bullet}$) denotes the Laplace transform with respect to coordinate x_2 and p is the Laplace transform variable counterpart of x_2 .

In the following application we will not consider other loads than those produced by the heat inputs (*i.e.*, we will assume $\hat{f}^M = 0$); thus, the thermal load vector. Assuming a constant heat flux in space and time, the thermal load vector may be written as

$$\hat{\tilde{f}}^T(p, s) = \sum_{m=0}^{\infty} p \hat{\tilde{U}}(m, p, s) \int_0^L [\mathbf{U}_1(m, x_2^*)\tilde{y}(x_2^*, s) + \mathbf{U}_2(m, x_2^*)\tilde{y}'(x_2^*, s)] dx_2^* \quad (26)$$

Denoting the first multiplicative term in Eq.(25) as

$$\hat{\tilde{\mathbf{H}}}(p, s, U) := \left[p^2\mathbf{K} + p\tilde{\mathbf{N}}(s, U) + \tilde{\mathbf{Q}}(s, U) \right]^{-1} \quad (27)$$

which can be regarded, apart from the boundary conditions, as the aeroelastic operator, and, using Eqs.(25) and (26), one may write the state-space vector for the particular problem of a heated wing in an incompressible flow field (Eq.(25)) as

$$\hat{\tilde{y}}(p, s) = \hat{\tilde{\mathbf{H}}}(p, s, U) \left\{ \sum_{m=0}^{\infty} p \hat{\tilde{U}}(m, p, s) \int_0^L [\mathbf{U}_1(m, x_2^*)\tilde{y}(x_2^*, s) + \mathbf{U}_2(m, x_2^*)\tilde{y}'(x_2^*, s)] dx_2^* + \mathbf{K}\tilde{y}'(0, s) \right\} \quad (28)$$

Applying the inverse Laplace transform with respect to space to Eq. (28) one has

$$\tilde{y}(x_2, s) = \sum_{m=0}^{\infty} \int_0^{x_2} \tilde{\mathbf{H}}(\eta, s) \tilde{\mathbf{U}}'(m, x_2 - \eta, s)$$

$$\left[\int_0^L \mathbf{U}_1(m, x_2^*)\tilde{y}(x_2^*, s) dx_2^* + \int_0^L \mathbf{U}_2(m, x_2^*)\tilde{y}'(x_2^*, s) dx_2^* \right] d\eta + \tilde{\mathbf{H}}(x_2, s, U) \mathbf{K}\tilde{y}'(0, s) \quad (29)$$

Introducing the following definition for the convolution integral

$$\tilde{\mathbf{g}}(x_2, s) := - \int_0^{x_2} \tilde{\mathbf{H}}(\eta, s) \tilde{\mathbf{U}}(m, x_2 - \eta, s) d\eta \quad (30)$$

and differentiating Eq.(29) with respect to the spanwise coordinate x_2 , one has

$$\tilde{y}'(x_2, s) = \sum_{m=0}^{\infty} \tilde{\mathbf{g}}'(m, x_2, s) \left[\int_0^L \mathbf{U}_1(m, x_2^*)\tilde{y}(x_2^*, s) dx_2^* + \int_0^L \mathbf{U}_2(m, x_2^*)\tilde{y}'(x_2^*, s) dx_2^* \right] + \tilde{\mathbf{H}}'(x_2, s, U) \mathbf{K}\tilde{y}'(0, s) \quad (31)$$

Thus, one may use the boundary condition at the tip (Eq.(10)), properly rewritten in the Laplace time-domain, to evaluate the unknown derivative $\tilde{y}'(0, s)$ appearing in the previous equations. Indeed, substituting Eqs.(29) and (31) in Laplace transformed counterpart of Eq.(10) one has

$$\begin{aligned} & \mathbf{R} \left\{ \tilde{\mathbf{H}}'(L, s) \mathbf{K}\tilde{y}'(0, s) + \sum_{m=0}^{\infty} \tilde{\mathbf{g}}'(m, L, s) \right. \\ & \left. \int_0^L [\mathbf{U}_1(m, x_2^*)\tilde{y}(x_2^*, s) + \mathbf{U}_2(m, x_2^*)\tilde{y}'(x_2^*, s)] dx_2^* \right\} \\ & + \mathbf{S} \left\{ \tilde{\mathbf{H}}(L, s) \mathbf{K}\tilde{y}'(0, s) + \sum_{m=0}^{\infty} \tilde{\mathbf{g}}(m, L, s) \right. \\ & \left. \int_0^L [\mathbf{U}_1(m, x_2^*)\tilde{y}(x_2^*, s) + \mathbf{U}_2(m, x_2^*)\tilde{y}'(x_2^*, s)] dx_2^* \right\} = \\ & = \sum_{m=0}^{\infty} \tilde{\mathbf{U}}(m, L, s) \int_0^L [\mathbf{U}_1(m, x_2^*)\tilde{y}(x_2^*, s) \\ & + \mathbf{U}_2(m, x_2^*)\tilde{y}'(x_2^*, s)] dx_2^* + \tilde{\mathbf{c}}_3(s) \end{aligned} \quad (32)$$

thus, the vector of unknown boundary conditions $(\tilde{y}'(0, s))$ may be written

$$\tilde{y}'(0, s) = - \left[\tilde{R}\tilde{H}'(L, s)K + \tilde{S}\tilde{H}(L, s)K \right]^{-1} \sum_{m=0}^{\infty} \left[\tilde{R}\tilde{g}'(m, L, s) + \tilde{S}\tilde{g}(m, L, s) - \tilde{U}(m, L, s) \right] \int_0^L [\mathbf{U}_1(m, x_2^*) \tilde{y}(x_2^*, s) + \mathbf{U}_2(m, x_2^*) \tilde{y}'(x_2^*, s)] dx_2^* \quad (33)$$

Introducing the following definitions

$$\tilde{W}(s) = \left[\tilde{R}\tilde{H}'(L, s)K + \tilde{S}\tilde{H}(L, s)K \right] \\ \tilde{V}(m, s) = - \left[\tilde{R}\tilde{g}'(m, L, s) + \tilde{S}\tilde{g}(m, L, s) - \tilde{U}(m, L, s) \right]$$

and substituting them in Eqs.(33) and in (29), one may obtain the closed form solution of the problem in the double transformed Laplace space time domain

$$\tilde{y}(x_2, s) = \tilde{H}(x_2, s)K \left\{ \tilde{W}^{-1}(s) \sum_{m=0}^{\infty} \tilde{V}(m, s) \int_0^L [\mathbf{U}_1(m, x_2^*) \tilde{y}(x_2^*, s) + \mathbf{U}_2(m, x_2^*) \tilde{y}'(x_2^*, s)] dx_2^* + \tilde{W}^{-1}(s) \tilde{c}_3(s) \right\} + \sum_{m=0}^{\infty} \tilde{g}(m, x_2, s) \\ \int_0^L [\mathbf{U}_1(m, x_2^*) \tilde{y}(x_2^*, s) + \mathbf{U}_2(m, x_2^*) \tilde{y}'(x_2^*, s)] dx_2^* \\ = \sum_{m=0}^{\infty} \left[\tilde{H}(x_2, s)K\tilde{W}^{-1}(s) \tilde{V}(m, s) + \tilde{g}(m, x_2, s) \right] \\ \int_0^L [\mathbf{U}_1(m, x_2^*) \tilde{y}(x_2^*, s) + \mathbf{U}_2(m, x_2^*) \tilde{y}'(x_2^*, s)] dx_2^* \\ + \tilde{H}(x_2, s)K\tilde{W}^{-1}(s) \tilde{c}_3(s) \quad (34)$$

Note that the state-space vector \tilde{y} appears not only in the left-hand side of Eq.(34) but also in its right handside under the integral sign.

Therefore, it is apparent that in order to solve this integral equation is it possible to employ a numerical approach, consisting either of an discretization of the integral either of an approximation of the vector of unknowns on a certain functional basis. In this paper a numerical discretization of the integral has been used to solve the coupled aero-thermo-elastic stability of the wing model. Specifically, the integrals in Eq.(34) may be discretized (using the theorem of integration

by parts in Eq. (36))

$$\int_0^L \mathbf{U}_1(m, x_2^*) \tilde{y}(x_2^*, s) dx_2^* \quad (35)$$

$$\simeq \sum_{k=0}^{N-1} \mathbf{U}_1(m, x_{2k}) \tilde{y}(x_{2k}, s) \Delta x_2 \\ \int_0^L \mathbf{U}_2(m, x_2^*) \tilde{y}'(x_2^*, s) dx_2^* \quad (36) \\ \simeq \mathbf{U}_2(m, L) \tilde{y}(L, s) - \sum_{k=0}^{N-1} \mathbf{U}_2'(m, x_{2k}) \tilde{y}(x_{2k}, s) \Delta x_2$$

where N is the number of points on which the integral has been discretized, and Δx_2 the step in x_2

$$N = \frac{L}{\Delta x_2} \quad (37)$$

Hence, Eq.(34) may be rewritten

$$\tilde{y}(x_{2k}, s) = \sum_{m=0}^{\infty} \left[\tilde{H}(x_{2k}, s)K\tilde{W}^{-1}(s) \tilde{V}(m, s) + \tilde{g}(m, x_{2k}, s) \right] \\ \left[\sum_{k=0}^{N-1} \mathbf{U}_1(m, x_{2k}) \tilde{y}(x_{2k}, s) \Delta x_{2k} + \mathbf{U}_2(m, L) \tilde{y}(L, s) - \sum_{k=0}^{N-1} \mathbf{U}_2'(m, x_{2k}) \tilde{y}(x_{2k}, s) \Delta x_{2k} \right] + \\ + \tilde{H}(x_{2k}, s)K\tilde{W}^{-1}(s) \tilde{c}_3(s) \quad (38)$$

Introducing the discrete vector of unknowns $\mathbf{Y}(s)$

$$\mathbf{Y}(s) = \{\tilde{y}(x_{20}, s), \tilde{y}(x_{21}, s), \dots, \tilde{y}(x_{2N}, s)\}^T \quad (39)$$

and defining the following matrix operators \mathbf{Z} , \mathbf{C}_1 , \mathbf{C}_2 , \mathbf{C}_3 , \mathbf{A} of dimension $4N \times 4N$ each

$$\tilde{\mathbf{Z}}(m, s) = \begin{bmatrix} \dots & & & \\ & \tilde{H}(x_{2k}, s)K\tilde{W}^{-1}(s) \tilde{V}(m, s) + \tilde{g}(m, x_{2k}, s) & & \\ & & \dots & \\ & & & \dots \end{bmatrix}$$

$$\mathbf{C}_1(m) =$$

$$\begin{bmatrix} \mathbf{U}_1(m, x_{20}) & \mathbf{U}_1(m, x_{2k}) & \mathbf{U}_1(m, x_{2(N-1)}) \\ \vdots & \vdots & \vdots \\ \mathbf{U}_1(m, x_{20}) & \mathbf{U}_1(m, x_{2k}) & \mathbf{U}_1(m, x_{2(N-1)}) \end{bmatrix}$$

$$\mathbf{C}_2(m) = \begin{bmatrix} 0 & \dots & \mathbf{U}_2(m, L) \\ \vdots & \vdots & \vdots \\ 0 & \dots & \mathbf{U}_2(m, L) \end{bmatrix}$$

$$\mathbf{C}_3(m) = \begin{bmatrix} \mathbf{U}_2'(m, x_{20}) & \mathbf{U}_2'(m, x_{2k}) & \mathbf{U}_2'(m, x_{2(N-1)}) \\ \vdots & \vdots & \vdots \\ \mathbf{U}_2'(m, x_{20}) & \mathbf{U}_2'(m, x_{2k}) & \mathbf{U}_2'(m, x_{2(N-1)}) \end{bmatrix}$$

$$\tilde{\mathbf{A}}(s) = \begin{bmatrix} \ddots & & & & & \\ & \ddots & & & & \\ & & \tilde{\mathbf{H}}(x_{2k}, s) \mathbf{K} \tilde{\mathbf{W}}^{-1}(s) & & & \\ & & & \ddots & & \\ & & & & \ddots & \\ & & & & & \ddots \end{bmatrix} \quad (40)$$

equation (38) becomes

$$\left\{ \mathbf{I} - \sum_{m=0}^{\infty} \tilde{\mathbf{Z}}(m, s) [\mathbf{C}_1(m) \Delta x_2 - \mathbf{C}_2(m) + \mathbf{C}_3(m) \Delta x_2] \right\} \tilde{\mathbf{Y}}(s) = \tilde{\mathbf{A}}(s) \tilde{\mathbf{F}}_3^T(s) \quad (41)$$

Finally, from the previous equation one obtains

$$\tilde{\mathbf{Y}}(s) = \left\{ \mathbf{I} - \sum_{m=0}^{\infty} \tilde{\mathbf{Z}}(m, s) [\mathbf{C}_1(m) \Delta x_2 - \mathbf{C}_2(m) + \mathbf{C}_3(m) \Delta x_2] \right\}^{-1} \tilde{\mathbf{A}}(s) \tilde{\mathbf{F}}_3^T(s) \quad (42)$$

It should be noticed that by discarding the components of the heat flux in the chordwise and spanwise directions, that implies that no thermo-mechanical coupling is involved, the previous equation provides the aeroelastic response in the Laplace transformed time domain of the wing, due to the application of an external heat flux in the thickness direction. [13, 14] Finally, note that the evaluation of the roots of the determinant of the matrix operator in brackets in Eq.(42) are the poles of the considered aerothermoelastic system. The evaluation of these poles at different flight speeds and different heat fluxes permits the determination of the domains of aero-thermo-elastic stability/instability of the wing. This analysis will be presented in the following section.

5. Numerical results

Goland's wing structural model (Ref. [24]) was considered as a reference configuration in Ref. [14] for the assessment and validation of the present aerothermoelastic model in the case of homogeneous material. In the following subsections the influence of the use of FGM materials for the aeroelastic performances (Subsection 5.1) and aerothermoelastic performances (Subsection 5.2) will be presented.

5.1. Aeroelastic analysis

The following wing geometrical characteristics have been used for the numerical applications:

$$\begin{aligned} L &= 6.0 \text{ m} \\ c &= 0.4 \text{ m} \\ t &= 0.02 \text{ m} \\ \Lambda &= 0 \text{ deg} \end{aligned}$$

where L is the mid-span, c the chord measured normally to the trailing edge and Λ is the swept angle. This wing geometry has been chosen instead of the Goland model in order to have and study a flutter instability for the FGM configuration considered within

the range of applicability of the used aerodynamic model. In particular, three models of wing have been

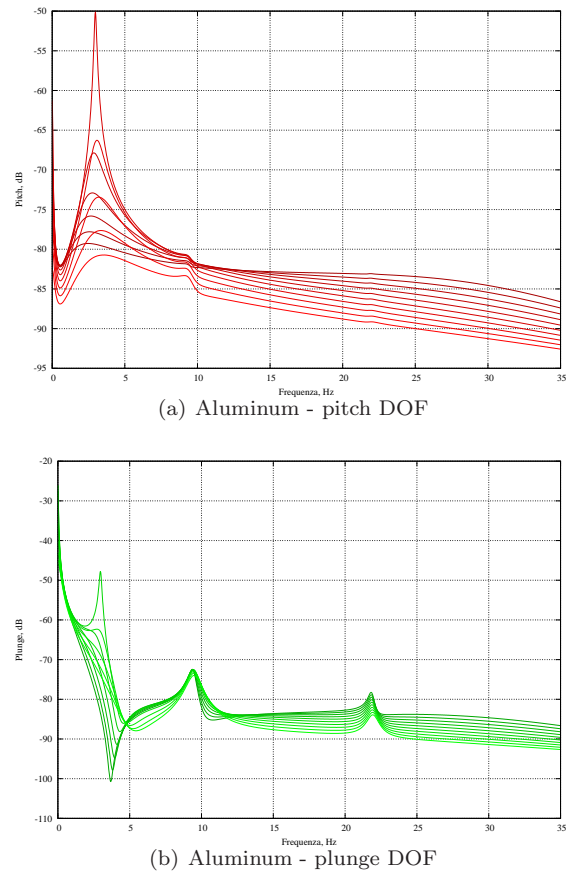


Figure 5. Aeroelastic responses using (homogeneous) aluminum

studied and compared in the following: one completely made of aluminum, and two made of FGM. The first FGM model has been chosen imposing the exponents n_u, n_l of Eq.(4) equals to 10 (see Fig. 3), and the second one putting them equals to 3. Indeed, for $n = 3$ the 50% of the two phases are present at about the 12.5% of thickness, whereas for $n = 10$ the 50% is found at about the 5% of thickness with aluminum placed in the wing core and alumina in the external layers of the wing. In other words, for $n = 3$ the amount of alumina is higher than for $n = 10$ and, in the limit, for $n \rightarrow \infty$ the pure aluminum configuration is achieved. In the following, these two FGM configurations will be referred as FGM 10 and FGM 3 respectively. Results of aeroelastic analysis are reported in Figs. 5, 6, and 7 where the frequency response function (FRF) for pitch θ and plunge h degrees of freedom at the wing tip are shown for the three configurations considered (aluminum, FGM 10 and FGM 3 respectively)

for several flight speeds in the neighbourhood of the corresponding flutter speed. The FRFs exhibit the flutter frequency in the abscissa of the highest peak in Figs. 5-7; frequency and flutter speed are summarized in Tab. 1. As expected, both flutter speed and frequency increase with the ceramic fraction of the FGM because the stiffness of alumina is higher than that of aluminum, although the relevant level of brittleness would not practically permit the achievement of such a performance. As general comment on these results it can be pointed out that, in the aeroelastic response point of view, the difference between aluminum and FGM behaviors are not so relevant.

5.2. Aerothermoelastic analysis

In this section an exact approach has been employed to solve the aerothermoelastic problem previously introduced. In Reference [12] Eq.(42) has been used directly to obtain the static/dynamic stability boundaries of the Goland's wing homogeneous model (Refs. [24,25]) with warping restraints included for different combinations of the heat density vector components (*i.e.*, for different directions of the perturbing heat density vector).

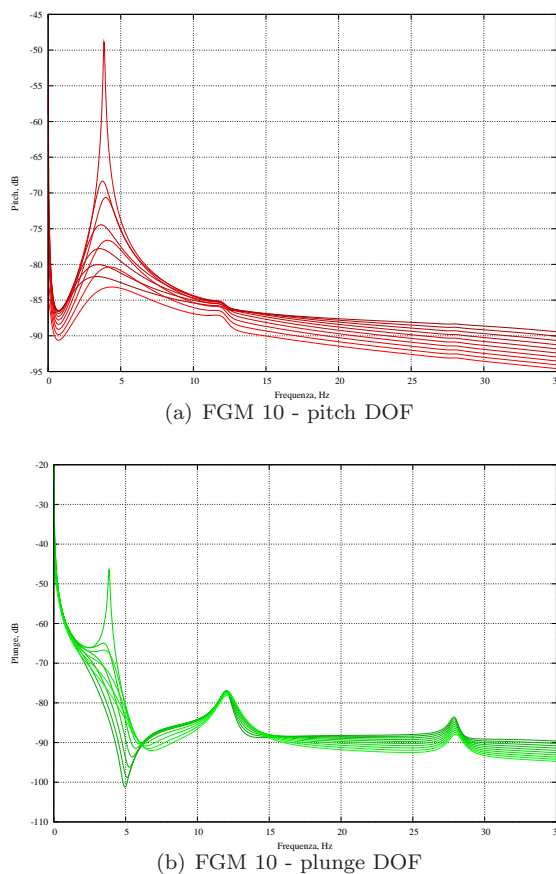
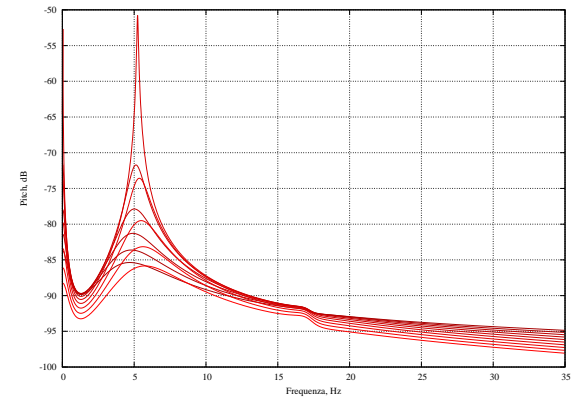
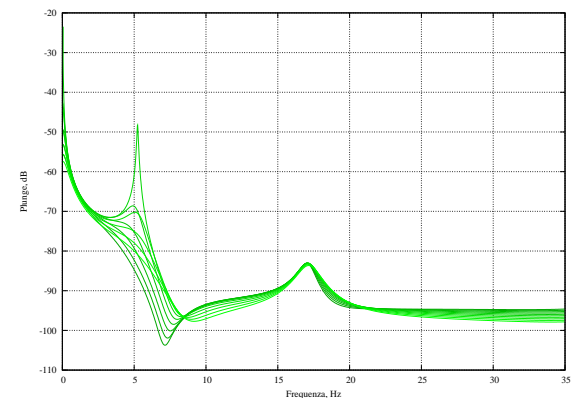


Figure 6. Aeroelastic responses using FGM 10



(a) FGM 3 - pitch DOF



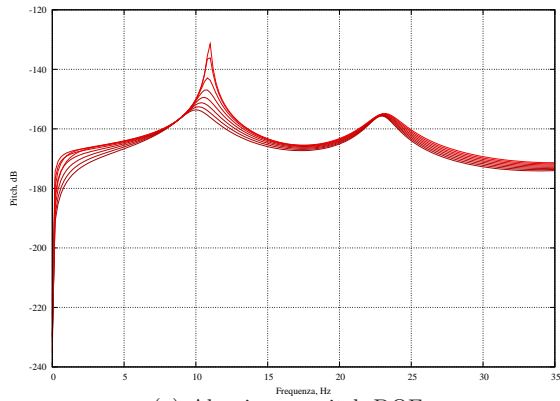
(b) FGM 3 - plunge DOF

Figure 7. Aeroelastic responses using FGM 3

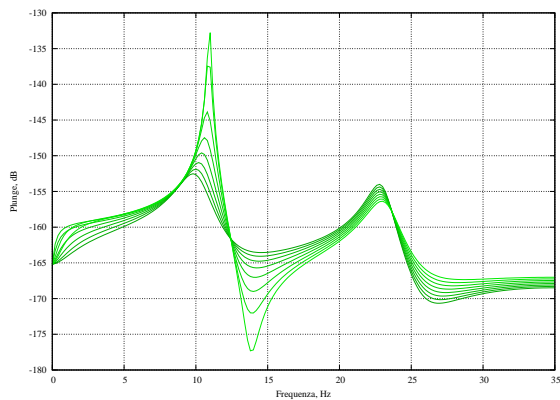
Here, Figure 8 shows the aerothermoelastic responses evaluated for the same FGM cases previously presented in Figs. 5-7: these Figures depict that the effect on the spectral content of the response due to thermal coupling is not negligible. One may also note that in this case the difference between aluminum and FGM in the aerothermoelastic response is much more pronounced than in the purely aeroelastic case.

6. Concluding remarks

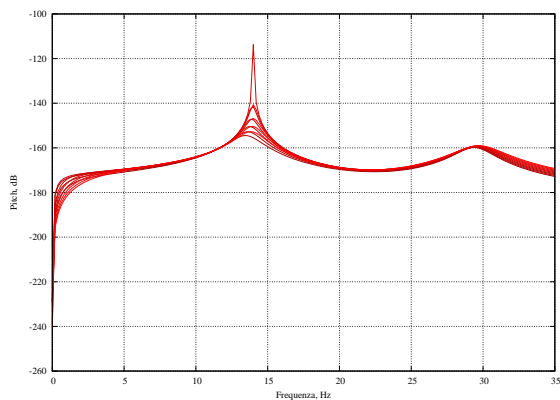
In this paper an exact aerothermoelastic analysis of swept wings realized by Functionally-Graded Materials, featuring non-classical structural effects, and impacted by a heat flux vector is presented. The aerothermoelastic model is coupled in the sense that the thermal loads are evaluated on the deformed configuration of the structure in a way similar to what is usually done in the aeroelasticity discipline. The theoretical model is completely developed and the exact analytical solution is obtained using a double Laplace transform technique. Moreover an analytical procedure to determine the thermal field on the Functionally-Graded Material solid as been proposed



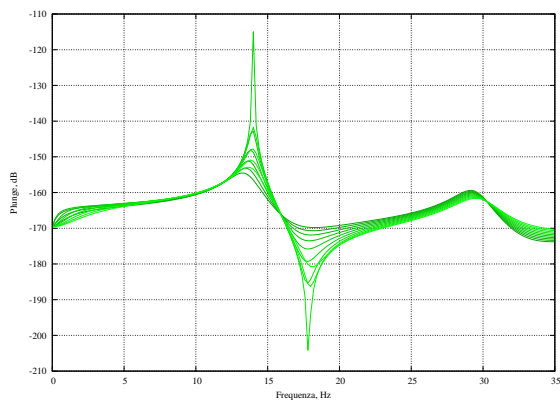
(a) Aluminum - pitch DOF



(b) Aluminium - plunge DOF



(c) FGM 10 - pitch DOF



(d) FGM 10 - plunge DOF

Figure 8. Aerothermoelastic response using homogeneous vs. FGM

Material	Flutter speed (m/s)	Flutter frequency (Hz)
Aluminum	92.0	3.0
FGM 10	120.8	3.8
FGM 3	173.0	5.6

Table 1
Flutter frequencies and speeds for the analyzed models

and used for the applications. The advantage on using FGM in term of stability and response performance of the system has been clearly shown. As a natural development of the present model, the thermal and the unsteady aerodynamic field could be considered to be coupled and in this context the problems of aerothermoelastic instability and response are addressed.

REFERENCES

1. Thuruthimattam, B. J., Friedmann, P. P., McNamara, J. J., and Powell, K., "Modeling Approaches to Hypersonic Aerothermoelasticity with Applications to Reusable Launch Vehicles," *44th AIAA/ASME/ASCE/AHS/ASC Structures, Structural Dynamics & Materials Conference, April 7th - 10th 2003.*, 2003, AIAA-2003-1967.
2. Friedmann, P., McNamara, J., Thuruthimattam, B., and Nydick, I., "Aeroelastic Analysis of Hypersonic Vehicles," *Journal of Fluids and Structures*, , No. 19, 2004, pp. 681–712.
3. McNamara, J. J., Thuruthimattam, B. J., Friedmann, P. P., and Powell, K., "Hypersonic Aerothermoelastic Studies for Reusable Launch Vehicles," *45th AIAA/ASME/ASCE/AHS/ASC Structures, Structural Dynamics & Materials Conference, April 19th - 22nd 2004.*, 2004, AIAA-2004-1590.
4. Thuruthimattam, B. J., Friedmann, P. P., McNamara, J. J., Powell, K. G., and Bartels, R. E., "A Computational Study of Vehicle Aeroelastic and Aerothermoelastic Behavior in Hypersonic Flow," *CEAS/AIAA/DGLR International Forum on Aeroelasticity and Structural Dynamics 2005, June 28th - July 1st 2005*, 2005, AIAA-200.
5. Boley, B. A. and Weiner, J. H., *Theory of Thermal Stresses*, John Wiley and Sons, 1960.
6. Augusti, G., "Instability of Struts Subject to Radiant Heat," *Meccanica*, Vol. 3, No. 2, 1968, pp. 167–176.
7. Yu, Y., "Thermally Induced Vibrations and Flutter of a Flexible Boom," *Journal of Spacecraft and Rockets*, Vol. 6, No. 8, 1969, pp. 902–910.
8. Manolis, G. and Beskos, D., "Thermally Induced Vibrations of Beam Structures," *Computer Methods in Applied Mechanics and Engineering*, Vol. 21, No. 3, 1980, pp. 337–355.
9. Thornton, E. A., *Thermal Structures for Aerospace Applications*, AIAA, 1996.
10. Blandino, J. R. and Thornton, E., "Thermally Induced Vibration of an Internally Heated Beam," *Journal of Vibration and Acoustics*, Vol. 123, 2001, pp. 67–75.
11. Garrick, I. E., "A Survey of Aerothermoelasticity," *Aerospace Engineering*, Vol. 22, No. 1, 1963, pp. 140–147.
12. Polli, G.M., Mastroddi, F., Librescu, L., Di Trapani,

- C., "Aerothermoelastic Stability of Composite Aerovehicle Wings Subjected to Heat Inputs," *Aiaa Journal*, Vol. 46, No. 4, April 2008.
13. Polli, G. M., Librescu, L., and Mastroddi, F., "Aeroelastic Response of Composite Aircraft Swept Wings Impacted by a Laser Beam," *AIAA Journal*, Vol. 44, No. 2, 2006, pp. 382–391.
 14. Argiolas, A., Mastroddi, F., and Polli, G. M. "Aerothermoelastic Response of a Functionally-Graded Aircraft Wing to Heat Loads," *49th AIAA/ASME/ASCE/AHS/ASC Structures, Structural Dynamics & Materials Conference, April 7th - 10th 2008.*, 2008, AIAA-2008-2018.
 15. Karpouzian, G. and Librescu, L., "Comprehensive Model of Anisotropic Composite Aircraft Wings Suitable for Aeroelastic Analyses," *Journal of Aircraft*, Vol. 31, No. 3, 1994, pp. 703–712.
 16. Gern, F. H. and Librescu, L., "Static and Dynamic Aeroelasticity of Advanced Aircraft Wings Carrying External Stores," *AIAA Journal*, Vol. 36, No. 7, 1998, pp. 1121–1129.
 17. Librescu, L. and Thangjitham, S., "Analytical Studies on Static Aeroelastic Behavior of Forward-Swept Composite Wing Structures," *Journal of Aircraft*, Vol. 28, No. 2, 1991, pp. 151–157.
 18. Karpouzian, G. and Librescu, L., "Nonclassical Effects on Divergence and Flutter of Anisotropic Swept Aircraft Wings," *AIAA Journal*, Vol. 34, No. 4, 1996, pp. 768–794.
 19. Polli, G. M., *Structural Modeling for Aerothermoelastic Analysis and Control*, Ph.D. thesis, School of Aerospace Engineering, University of Rome "La Sapienza", 2005.
 20. Fung, Y. C., *An Introduction to the Theory of Aeroelasticity*, Dover, 1969.
 21. Bisplinghoff, R. L. and Ashley, H., *Principles of Aeroelasticity*, John Wiley and Sons, 1962.
 22. Librescu, L., "Aeronautical and Mechanical structural systems made-up of FGM: modeling and behaviour" *Lecture held in Rome*, University of Rome *La Sapienza*, 2006.
 23. Carlson, D. E., "Linear Thermoelasticity," *Encyclopedia of Physics*, edited by C. Truesdell, Vol. VIa/2, Springer-Verlag, Berlin, 1972, pp. 297–345.
 24. Goland, M., "The Flutter of a Uniform Cantilever Wing," *Journal of Applied Mechanics*, Vol. 12, No. 4, 1945, pp. A197–A208.
 25. Goland, M. and Luke, Y. L., "The Flutter of a Uniform Wing With Tip Weights," *Journal of Applied Mechanics*, Vol. 15, No. 1, 1948, pp. 13–20.